A COMPARATIVE STUDY OF RADAR STEREO AND INTERFEROMETRY FOR DEM GENERATION[*]

M. Gelautz[(1)], P. Paillou[(2)], C. W. Chen[(3)], H. A. Zebker[(4)]

[(1)] *Vienna University of Technology, Favoritenstrasse 9-11/188/2, A-1040 Vienna, Austria, Email: gelautz@ims.tuwien.ac.at*
[(2)] *Observatoire Aquitain des Sciences de l'Univers, 2 rue de l'observatoire, BP 89, 33270 Floirac, France, Email: paillou@obs.u-bordeaux1.fr*
[(3)] *JPL, 4800 Oak Grove Dr, MS 300-235, Pasadena, CA 91109-8099, United States, Email: Curtis.W.Chen@jpl.nasa.gov*
[(4)] *Stanford University, 334 Packard Electrical Engineering, Mail Code 9515, Stanford, CA 94305-9515, United States, Email: zebker@stanford.edu*

ABSTRACT

In this experiment, we derive and compare radar stereo and interferometric elevation models (DEMs) of a study site in Djibouti, East Africa. As test data, we use a Radarsat stereo pair and ERS-2 and Radarsat interferometric data. Comparison of the reconstructed DEMs with a SPOT reference DEM shows that in regions of high coherence the DEMs produced by interferometry are of much better quality than the stereo result. However, the interferometric error histograms also show some pronounced outliers due to decorrelation and phase unwrapping problems on forested mountain slopes. The more robust stereo result is able to capture the general terrain shape, but finer surface details are lost. A fusion experiment demonstrates that merging the stereoscopic and interferometric DEMs by utilizing coherence-derived weights can significantly improve the accuracy of the computed elevation maps.

1 INTRODUCTION

Radar stereogrammetry and interferometry are two of the different approaches for generating Digital Elevation Models (DEMs) from radar images [6]. Of the two methods, stereo analysis presents the more traditonal approach. One of the major goals of early radar stereo studies was to better understand the extent to which the principles and methods of conventional optical stereo analysis could be applied successfully to radar imagery. A detailed discussion of the radar stereo geometry and related applications can be found in [3]. Research in radar interferometry was strongly stimulated by the launch of ESA's ERS-1 satellite in 1991. Studies have demonstrated the potential of the interferometric technique to produce high-resolution topographic maps with relative height errors of 5m or less, as found by [7] in tests with 3-day repeat-pass ERS-1 imagery.

From the geometric point of view, an interferometric pair can be regarded as a stereo pair with a very small intersection angle (or baseline). However, it should be noted that viewing angle differences usable for same-side stereo analysis typically range from around 5° to 45° and are thus on a different order of magnitude than baselines for interferometric studies. In both stereo and interferometry, larger baselines improve the vertical height resolution. However, increasing baselines lead also to stronger dissimilarities between the two images at the wavelength/pixel level, which make the phase unwrapping/matching process more difficult. The selection of an optimal stereoscopic or interferometric viewing geometry for a given application must be based on a compromise between these competing effects, with the due consideration given to the local topography and scene content.

The goal of our study is to compare the performance of radar stereo and interferometry in application to a common test site. Most related studies on DEM generation have employed either stereo or interferometry exclusively, and therefore do not provide a direct comparison of the two techniques in response to one and the same terrain characteristics. In particular, our study is motivated by the growing availability of spaceborne stereo data delivered by the multi-look angle capabability of ESA's Envisat satellite and Canada's Radarsat program, which complement the interferometric data sets provided by these and other sensors (e.g., ERS-2).

---

[*] An extended version will appear in *International Journal of Remote Sensing*.

2 DATA SET

Our test site is the Asal Rift, an arid volcanic region in the Republic of Djibouti, East Africa. The site includes both relatively flat, homogeneous regions as well as forested mountain slopes and terrain discontinuities. Thus, the area contains features that are expected to strain both the stereo matching and interferometric phase unwrapping. For stereo analysis, we use a same-side Radarsat image pair that was acquired with a stereo intersection angle of 9°. The stereo data are shown in Fig. 1. Our interferometric data set consists of a Radarsat interferometric pair with a temporal baseline of 24 days and an ERS-2 interferometric pair that was taken with an acquisition interval of 35 days. The corresponding height ambiguities are 54m (Radarsat) and 17m (ERS-2). All images were resampled to a ground resolution of approximately 20m in both dimensions. Fig. 2 shows the ERS-2 interferogram along with the corresponding magnitude image and coherence map.

For evaluation, we used a reference DEM that was derived from optical SPOT stereo images. The DEM has an estimated accuracy of 7m – 10m. It should be noted that our error analysis in section 4 concentrates on pronounced interferometric errors on the order of several phase cycles for which the SPOT DEM – despite its limited usefulness for high-precision interferometric evaluation – presents a valid reference.
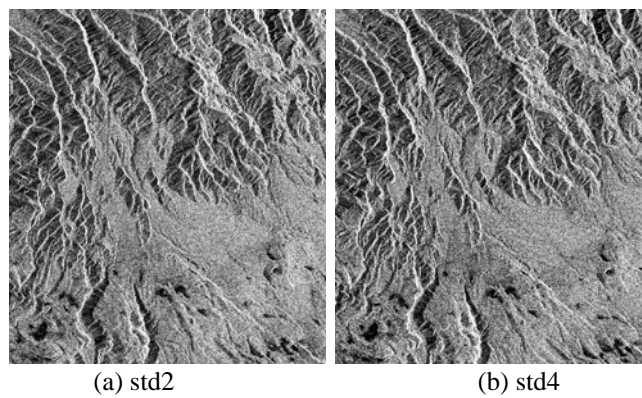

(a) std2   (b) std4

Fig. 1. Radarsat stereo image pair acquired from the right with look angles of 28° (a) and 37° (b).
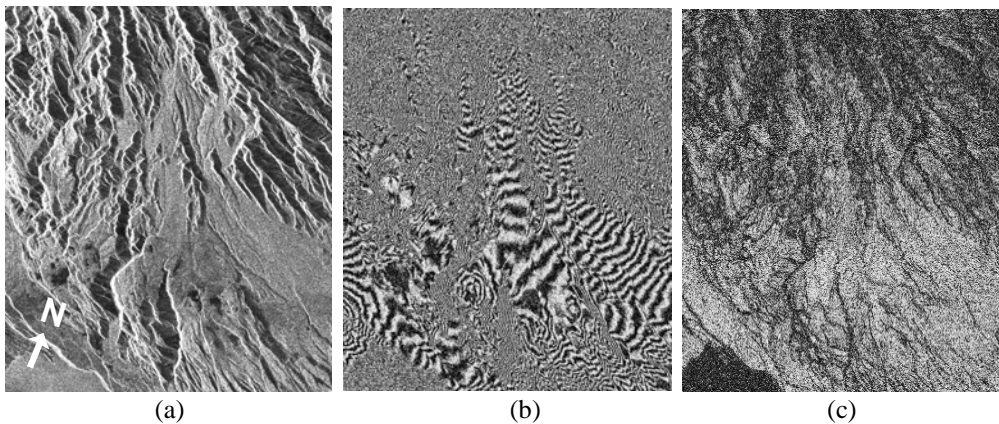

(a)   (b)   (c)

Fig. 2. ERS-2 interferometric data set: (a) magnitude image, (b) interferogram, (c) coherence map.

3 ALGORITHMS

The key steps in stereo and interferometric analysis are stereo matching and interferometric phase unwrapping, respectively. For automated stereo matching, we employed a hierarchical correlation-based approach described by [2] in

combination with a pre-processing step that enhances relief-induced edges [4]. Output of the matcher was a grid of match points located 8 pixels apart, which corresponds to a nominal spacing of 160m on the ground. We used a confidence value derived from the shape of the correlation surface to filter out match points with low reliability. It should be noted that the ability of radar stereo to capture surface details cannot be refined arbitrarily by simply increasing the match point density. We carried out additional tests with finer grid sizes and did not observe any significant changes of the results. The match points were converted into terrain height by using the stereo intersection module of the RSG software package [5].

We unwrapped the interferogram using the dynamic-cost cycle-cancelling (DCC) technique proposed by [1]. The DCC algorithm provides global coverage and allows the incorporation of user-defined weights. For topographic applications, meaningful weights are derived from edges in the amplitude image, which suggest the occurrence of terrain discontinuities. After projection into the DEM geometry, a Delauney triangulation with bilinear interpolation was utilized to fill in missing elevation data due to undersampling of the terrain in foreshortening and layover regions.

We implemented a fusion algorithm that merges the stereo and interferometric DEMs by computing a weighted average. The weights were derived from a filtered coherence map along with user-defined threshold values. In regions with reliable interferometric results, the stereo information was completely discarded. On the other hand, in strongly decorrelated areas, the best results were obtained by using only the stereo DEM.

4 EXPERIMENTAL RESULTS

The quality of the reconstructed DEMs was assessed by comparison with the SPOT reference DEM. We computed the corresponding difference DEMs and analysed the resulting error histograms, as shown in Fig. 3. The dotted line in Fig. 3 gives the error distribution of the Radarsat stereo DEM, for which an error standard deviation of 45m was found. Comparison with the ERS-2 interferometric reconstruction (dashed line) shows the higher quality of the interferometric result as indicated by the higher central peak of the InSAR histogram. However, the interferometric reconstruction is corrupted by outliers which account for points in the outer regions of the histogram. These pronounced interferometric errors can be attributed to phase unwrapping errors in regions of low coherence caused by vegetated mountain slopes. Contrarily, the rounded shape of the stereo histogram reflects the lower accuracy but greater robustness of the stereo approach.
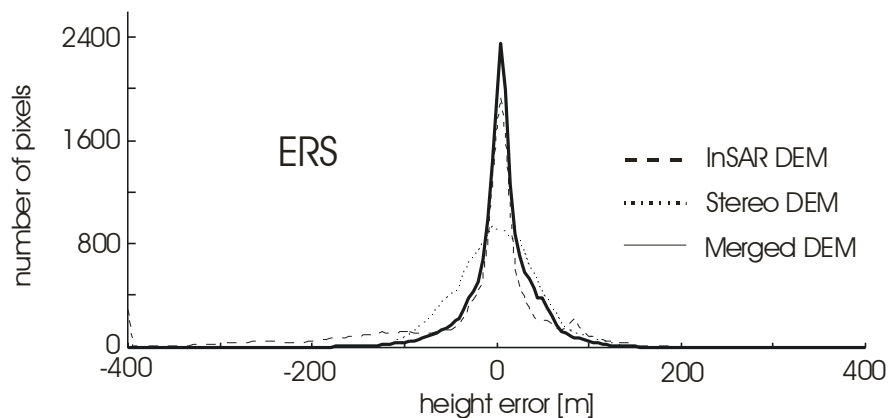

Fig. 3. Error histograms of the Radarsat stereo, ERS-2 interferometric, and merged DEMs.

The result of merging the interferometric and stereoscopic DEMs by using coherence-derived weights is represented by the solid curve in Fig. 3. In the central part of the histogram, the fusion DEM follows the high-quality interferometric reconstruction (dashed curve) and exhibits an even higher peak than the original curve. At the same time, the former interferometric outliers in the histogram wings were suppressed with the use of the Radarsat stereo data (dotted curve). Similar results were obtained when combining the Radarsat stereo DEM with the Radarsat interferometric DEM (not shown in Fig. 3).

The improvement achieved by merging was confirmed by the quantitative analysis in table 1, which gives a closer look at the cumulative error values in the histogram wings. The table entries focus on error values of 25m or more, for which the SPOT DEM presents a valid reference. One can recognize that in both the ERS-2 and Radarsat case the fusion DEM exhibits a significantly lower error rate than the stereo or corresponding interferometric DEM individually, which demonstrates again the usefulness of the merging approach.

Table 1. Reconstruction errors of stereoscopic, interferometric, and merged DEMs.

DEM	reconstruction error [%]					
	>25m	>50m	>75m	>100m	>150m	>200m
Stereo	56.7	26.0	10.1	3.5	0.2	0.0
InSAR (Radarsat)	24.4	12.6	10.2	9.3	8.0	6.9
Merged DEM (Radarsat)	21.6	6.9	3.0	1.2	0.1	0.0
InSAR (ERS-2)	47.1	33.4	25.8	18.7	10.7	6.8
Merged DEM (ERS-2)	34.8	14.4	5.5	2.1	0.2	0.0

Another look at the reconstruction errors is given by the scatter plots in Fig. 4. Subfigure (a) shows the ERS-2 interferometric height errors as a function of the filtered coherence values. One can recognize that larger height errors tend to be associated with lower coherence values, which indicates the usefulness of the interferometric coherence as a quality measure for subsequent merging. For comparison, the relationship between the Radarsat stereoscopic height errors and the ERS-2 interferometric coherence is shown in Fig. 4 (b). As expected, the two values appear to be highly uncorrelated. The merging result is shown in Fig. 4 (c). A comparison of the plots confirms again that the fusion process successfully substituted the more robust stereo measurements for the most severe interferometric errors.

5 CONCLUSIONS

In our tests, we found that in areas of high coherence the interferometric reconstruction clearly outperformed the stereo result. The generally smoother stereo reconstruction with an error standard deviation of 45m was able to capture the general terrain shape, but finer surface details were lost. Some forested mountain slopes led to pronounced outliers in the interferometric DEM due to low coherence and related phase unwrapping problems. In a fusion experiment, we demonstrated that merging the stereoscopic and interferometric DEMs by using weights derived from a filtered coherence map can significantly improve the accuracy of the computed elevation maps

In this study, we have concentrated primarily on interferometric height errors caused by decorrelation and resulting meaningless phase values. A possible topic for future research would be to investigate other phenomena such as atmospheric artefacts and orbital inaccuracies, along with the development of suitable interferometry-stereo fusion techniques that suppress these arrors.
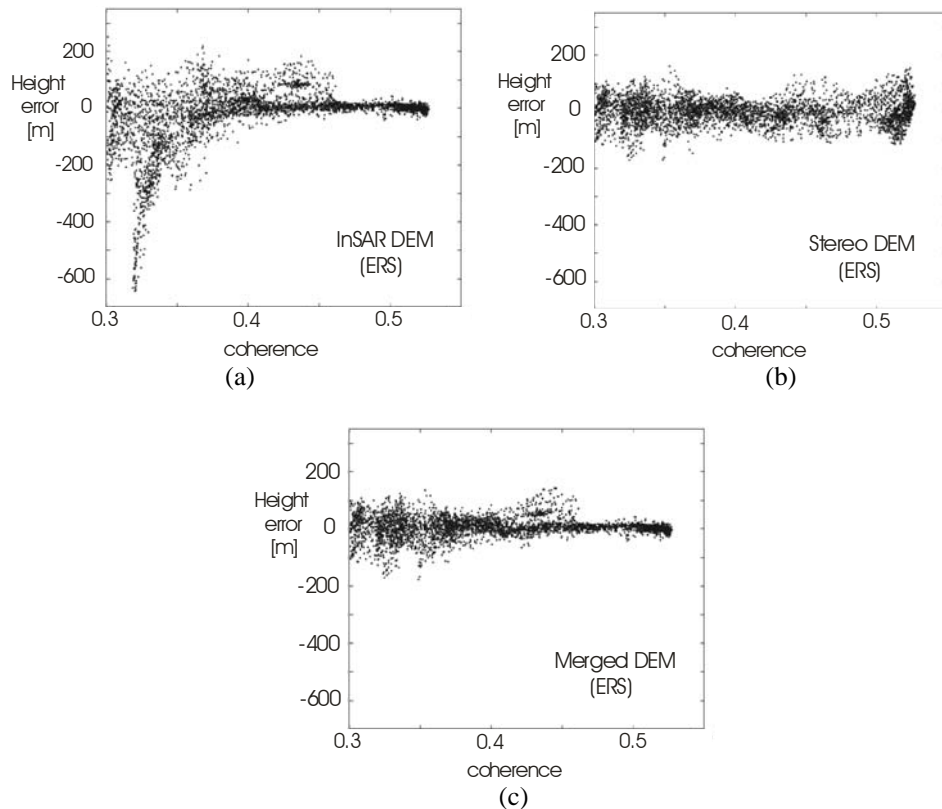
Fig. 4. Height error versus ERS-2 interferometric coherence for (a) ERS-2 interferometric DEM, (b) Radarsat stereo DEM, and (c) ERS-2/Radarsat merged DEM.

REFERENCES

1. Chen, C., and Zebker, H., 2000, Network approaches to two-dimensional phase unwrapping: intractability and two new algorithms. *Journal of the Optical Society of America A*, 17, 401-414.
2. Frankot, R., Shafer, S., and Hensley, S., 1994, Noise resistant estimation technique for SAR image registration and stereo mapping. *Proceedings IGARSS'94*, Pasadena, CA, August 1994 (New Jersey: IEEE Publications), 1151-1153.
3. Leberl, F., 1990, *Radargrammetric Image Processing*, 1st edn (Norwood, MA: Artech House).
4. Paillou, P., and Gelautz, M., 1999, Relief reconstruction from SAR stereo pairs: the "optimal gradient" matching method. *IEEE Transactions on Geoscience and Remote Sensing*, 37, 2099-2106.
5. RSG, 1993, *Remote Sensing Software Package Graz.* Software User Manual, 3rd edn, Institute for Digital Image Processing, JOANNEUM RESEARCH, Graz, Austria.
6. Toutin, T., and Gray, L., 2000, State-of-the-art of elevation extraction from satellite SAR data. *ISPRS Journal of Photogrammetry and Remote Sensing*, 55, 13-33.
7. Zebker, H., Werner, C., Rosen, P., and Hensley, S., 1994, Accuracy of topographic maps derived from ERS-1 interferometric radar. *IEEE Transactions on Geoscience and Remote Sensing*, 32, 823-836.